Differential Detection of Phospholipid Fluidity, Order, and Spacing by Fluorescence Spectroscopy of Bis-pyrene, Prodan, Nystatin, and Merocyanine 540

Heather A. Wilson-Ashworth,† Quinn Bahm,* Joshua Erickson,† Aaron Shinkle,† Mai P. Vu,* Dixon Woodbury,* and John D. Bell*

*Department of Physiology and Developmental Biology, Brigham Young University, Provo, Utah 84602; and †Department of Biology, Utah Valley State College, Orem, Utah 84058

ABSTRACT The properties of liquid-ordered, solid-ordered, and liquid-disordered phases were investigated by steady-state fluorescence spectroscopy in liposomes composed of mixtures of dipalmitoylphosphatidylcholine and cholesterol (0–40 mol %) as a function of temperature (24–51°C). The fluorescent probes used (bis-pyrene, nystatin, prodan, and merocyanine) were chosen because they differ in the location they occupy in the membrane and in the types of properties they sense. Comparison of phase diagrams with contour plots of the fluorescence data suggested that bis-pyrene is sensitive primarily to lipid order. In contrast, nystatin fluorescence intensity responded to changes in lipid fluidity. The shape of the prodan emission spectrum detected both liquid-solid and order-disorder transitions in the phase diagram. Merocyanine's behavior was more complex. First, it was more sensitive than any of the other probes to the membrane pretransition that occurs in the absence of cholesterol. Second, regardless of whether emission intensity, anisotropy, or spectral shape was observed, the probe appeared to distinguish two types of liquid-ordered phases, one with tightly packed lipids and one in which the apparent spacing among lipids was increased. The prodan data supported these results by displaying modest versions of these two observations. Together, the results identify eight regions within the phase diagram of distinguishable combinations of these physical properties. As an example of how this combined analysis can be applied to biological membranes, human erythrocytes were treated similarly. Temperature variation at constant cholesterol content revealed three of the eight combinations identified in our analysis of liposomes.

INTRODUCTION

Recently, there has been elevated interest in detecting and understanding membranes that display the properties of a liquid-ordered phase. This attention is the result of evidence suggesting the existence of specialized domains in cell membranes called lipid rafts. These rafts are enriched in cholesterol and sphingomyelin, behave physically as liquid-ordered structures, and are proposed to participate in various physiological functions (reviewed in Barenholz (1)).

Fluorescence spectroscopy has been employed extensively to study bilayer properties in both artificial and biological membranes. Several fluorescent probes are able to distinguish solid and fluid phases. Studies of liquid-ordered phases are more complex in that they depend on the ability of a probe to distinguish between membrane fluidity (lipid translational mobility) and phospholipid chain order. Since these two properties generally co-vary across thermotropic phase transitions, much of the previous use of fluorescent probes has not provided sufficient evidence to evaluate their utility for investigating liquid ordered phases. One means of addressing this situation was identified previously in experiments comparing the behavior of the probe Laurdan toward membranes displaying solid-ordered, liquid-disordered, or liquid-ordered phases. These experiments demonstrated that dual measurements of Laurdan anisotropy and emission spectra could successfully detect liquid-ordered structures in artificial bilayers and in biological membranes during experimental treatments (2).

The value of the approach with Laurdan was the use of different measurements that distinguished changes in lipid order from changes in fluidity (2). In this study, we have expanded the approach using a range of fluorescent probes (bis-pyrene, nystatin, prodan, and merocyanine 540) that differ in the location they occupy in the membrane and in the physical properties they sense (lipid order, fluidity, and packing). Dipalmitoylphosphatidylcholine (DPPC) liposomes were examined using these probes at a range of temperatures (ambient to 50°C) and cholesterol concentrations (0–40 mol %) to gain additional insights regarding the properties of different regions of the corresponding phase diagram. Furthermore, we applied the strategy to analysis of human erythrocyte membrane properties as a function of temperature.

Bis-pyrene consists of two pyrene molecules linked by a three-carbon spacer. It is reported to be highly sensitive to viscosity changes at the level of the fatty acid chains in the phospholipid bilayers (3,4). When the environment of the probe restricts lateral movement of the two pyrene moieties, fluorescence emission originates primarily from noninteracting pyrene monomers (370–400 nm). In contrast, when

Submitted June 7, 2006, and accepted for publication August 31, 2006.

Address reprint requests to John D. Bell, 302C WIDB, Brigham Young University, Provo, UT 84602. Tel.: 801-422-2353; Fax: 801-422-0050; E-mail: john_bell@byu.edu.

0006-3495/06/12/4091/11 $2.00

doi: 10.1529/biophysj.106.090860

lateral diffusion is unrestricted, the pyrene monomers interact with high probability, resulting in an emission spectrum dominated by excimer fluorescence (480 nm).

Nystatin is a polyene antibiotic containing a tetraene chromophore. Nystatin partitions much better (fivefold increase in partition coefficient) when the membrane is in a solid compared to liquid phase (5). The enhanced partitioning appears to represent relocation of nystatin from a position superficial in the membrane and parallel to the interface to one deep in the bilayer and parallel to the phospholipid chains (6). This deeply inserted configuration of the probe also corresponds to increased fluorescence intensity and a long excited-state lifetime, presumably due to limited ability of the probe to relax from the excited state through nonradiative changes in intramolecular vibrations. Alternatively, when the probe is present at the membrane interface or in bulk solution, constraints on such vibrational freedom are absent, and the intensity and lifetime therefore decrease (6).

Prodan contains the same fluorophore as Laurdan with the one difference being the length of the alkyl tail on the molecule (propyl instead of lauryl) (7). Consequently, prodan binds less tightly to the membrane than does Laurdan, and the probe therefore occupies a position more superficial in the headgroup region than Laurdan (which resides near the glycerol backbones) (8–10). The excited-state dipole of these probes is especially sensitive to solvent effects, and a large shift in emission maximum is therefore observed when the environmental polarity of the probe changes (7). Thus, the probe readily detects the membrane phase transitions (10).

Merocyanine 540 (MC540) is a heterocyclic chromophore with a localized negative charge that binds superficially to the outer leaflet of membranes (11–13). Several investigations in model membranes have demonstrated that its fluorescence characteristics are sensitive to subtle differences in lipid packing (14–18). When membrane lipids are tightly packed, MC540 assumes an orientation perpendicular and superficial to the phospholipid chains (emission maximum around 624 nm). When the lipids are less tightly packed, the emission maximum occurs at shorter wavelengths (~594 nm) with an increase in relative quantum yield (14,19). This higher-intensity emission appears to correspond to a reorientation of the dye to a position parallel to and immersed among the phospholipid chains (16).

MATERIALS AND METHODS

DPPC was purchased from Avanti Polar Lipids (Birmingham, AL). Choesterol was obtained from Spectrum (Gardena, CA) and ergosterol from Sigma-Aldrich. Prodan, MC540, diphenylhexatriene, and bis-pyrene, were acquired from Molecular Probes (Eugene, OR (now Invitrogen)) and nystatin was from Sigma (St. Louis, MO). Human erythrocytes were obtained from blood samples remaining after physical exams at the Brigham Young University Student Health Center. For experiments, cells were washed and suspended in a balanced salt medium as described previously (20).

To form liposomes, cholesterol and DPPC were dissolved in chloroform and mixed at the mole ratios indicated in the figures. The total lipid concentration (after reconstitution in aqueous buffer as liposomes) was 1 mM. Fluorescent probes were included with the lipids in the chloroform mixture (1.5 μM bis-pyrene, 4.3 μM nystatin, 7 μM MC540, or 20 μM prodan). The solvent was removed by evaporation under a nitrogen stream at room temperature and the lipids were hydrated at 50°C in 150 mM KCl, 20 mM sodium citrate/citric acid buffer (pH 7.0) by periodic vigorous agitation on a vortex mixer. This procedure yielded multilamellar vesicles. Ideally, the probe/lipid ratio would be 1:200 or less to minimize the potential for perturbation to membrane properties. Prodan and MC540 were at concentrations higher than this because the probes do not bind well to membranes, especially at low temperature. The fact that both probes detected the pretransition (see Figs. 5 and 6) and that prodan identified a sharp main transition (see Fig. 5) placates the concern. In any case, the purpose of this study was focused on comparing properties of different regions of the phase diagram rather than identifying exact phase boundaries.

Steady-state fluorescence emission was monitored with a Fluoromax (Jobin Yvon, Edison, NJ) or PC-1 (ISS, Champaign, IL) photon-counting spectrofluorometer. Temperature was controlled by a circulating water bath and sample homogeneity was maintained by continuous magnetic stirring. Samples were equilibrated in the fluorometer at 25°C. Emission spectra were collected at wavelengths appropriate for each probe (prodan: excitation 350 nm, emission 360–600 nm; bis-pyrene: excitation 344 nm, emission 360–600 nm; nystatin: excitation 315 nm, emission 325–550 nm; MC 540: excitation 540 nm, emission 550–700 nm). Band pass was set between 4 and 8 nm depending on the instrument and sample intensity. After acquiring data at 24–25°C, temperature was raised by 1–2°C, the sample reequilibrated, and fluorescence data again acquired. The process was repeated until reaching 50–51°C. To assess reversibility, data from the same sample were then obtained after returning the temperature to 25°C. Under the conditions used, interference from scattered light was negligible.

Data from bis-pyrene were quantified by calculating the excimer (479–488 nm)-to-monomer (394–397 nm) ratio. Nystatin results were evaluated by integration of the emission intensity at 404–412 nm. Prodan emission spectra were represented by the three-wavelength generalized polarization (3WGP), as described by Krasnowska et al. (10). Merocyanine 540 emission spectra were similarly assessed using the ratio of intensity at 583–587 nm and 619–623 nm.

The fluorescence emission of each probe was assessed at multiple temperatures between 24 and 51°C in vesicles containing 0–40 mol % cholesterol. Contour plots were generated by graphing the relevant fluorescence parameter as the z axis with temperature along the y axis and cholesterol concentration on the x axis. Plots are oriented with the z axis perpendicular to the plane of the paper. Contour lines represent incremental fluorescence parameter values. A theoretical DPPC/cholesterol phase diagram is superimposed on each contour plot for identification of phase boundaries.

Steady-state MC540 anisotropy measurements were obtained in the L-format using a PC-1 fluorometer from ISS (Champaign, IL) equipped with Glan-Thompson polarizers and 16-nm band pass on both monochromators. Samples were prepared as described above for steady-state emission intensity. Fluorescence intensity (MC540: excitation 540 nm, emission 585 nm; diphenylhexatriene: excitation 350 nm, emission 452 nm) was measured with excitation and emission polarizers parallel to each other (both at 0°, I_0) and repeated with the polarizers perpendicular (excitation 0°, emission 90°, I_{90}). Anisotropy was calculated using the traditional equation

$$r = \frac{I_0 - GI_{90}}{I_0 + 2GI_{90}}. \quad (1)$$

The correction factor (G) was obtained from the ratio of emission intensity at 0 and 90° with the excitation polarizer oriented at 90°. For the anisotropy experiments involving diphenylhexatriene, washed human erythrocytes (see Jensen et al. (20) for details) were incubated with the probe (2.5 μM final concentration with ~3×10^6 cells/ml) at least 30 min at room temperature before initiating data acquisition. Centrifugation experiments estimated that at this concentration of probe, the probe/lipid ratio is ~1:30. This relatively high ratio is necessary with erythrocytes to provide adequate

signal for measurements with polarized light while apparently not affecting erythrocyte structure (see comparisons with Laurdan (21, 22)) Background data (to account for scattered light) was obtained before adding probe and subtracted from the data before calculating the anisotropy values. Nevertheless, the contribution from scattered light was negligible.

RESULTS

Fig. 1 *A* displays the differences in the bis-pyrene emission spectrum at low and high temperatures. When the membrane was in the solid-ordered (S_O, also abbreviated L_β in many studies) phase (25°C), the spectrum reflected monomer fluorescence exclusively (~370–420 nm, *solid curve*). As expected, excimer fluorescence dominated when the membrane was in the liquid-disordered (L_α) phase (50°C, centered at 480 nm, *dashed curve*). The detailed effect of temperature on the ratio of bis-pyrene excimer and monomer fluorescence intensity in liposomes is shown in Fig. 1 *B*; the ratio increased as a function of temperature with the largest increases occurring near the membrane main phase transition (41.5°C). The presence of cholesterol in the membrane altered the ratio so that the prevalence of excimer fluorescence at high temperature was greatly reduced compared to control vesicles (Fig. 1 *C*). To interpret these results in the context of membrane phases, we generated a contour plot of the data of Fig. 1 *C* and superimposed on it a theoretical phase diagram of DPPC and cholesterol (23) (Fig. 2). The lines of the contour plot appeared roughly parallel with boundaries between ordered (liquid-ordered (L_O) and S_O) and disordered (L_α) phases.

In the case of nystatin, membrane phase was detected by probe emission intensity, as reported previously (5). High emission intensity was observed at 25°C. The effects of temperature and cholesterol concentration on nystatin fluorescence intensity are illustrated in Fig. 3 *A*. In contrast to the observations with bis-pyrene, nystatin fluorescence was altered by cholesterol more at low temperature than at high. This result translated into a contour plot containing lines parallel with transitions between solid and fluid phases (Fig. 3 *B*).

The primary effect of temperature on the prodan emission spectrum was a change in spectral shape (Fig. 4 *A*), consistent with the solvent relaxation effect and earlier observations (10). At low temperature, when phospholipids were in the S_O phase, the spectrum contained two peaks, one

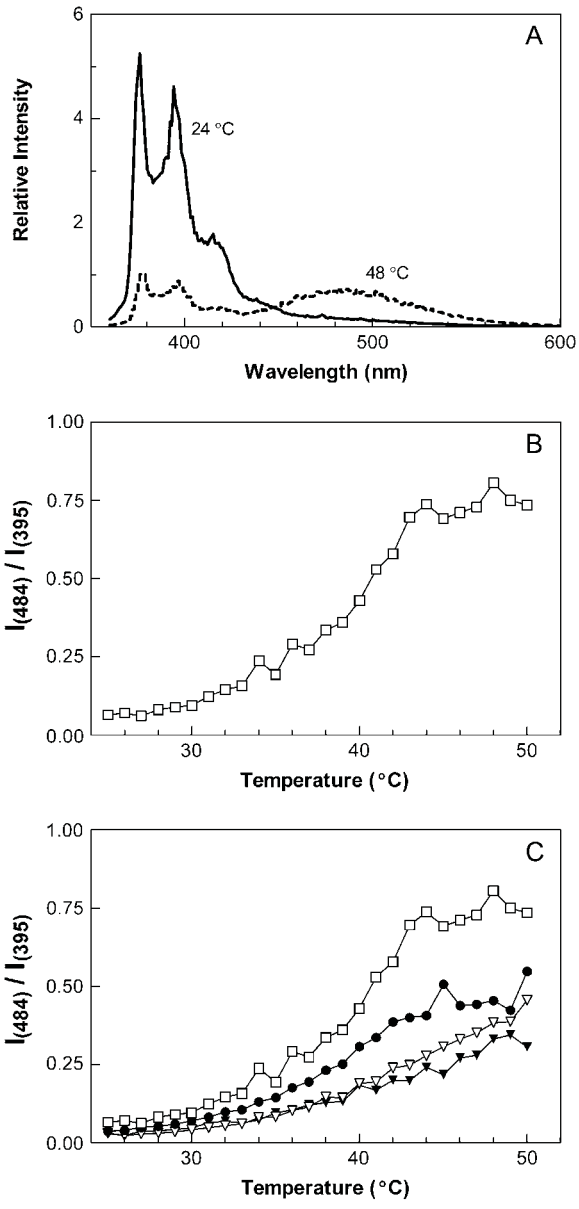

FIGURE 1 Effects of cholesterol content and temperature on bis-pyrene fluorescence. (*A*) The bis-pyrene emission spectrum in liposomes composed of 100% DPPC at 24°C (*solid curve*) and at 48°C (*dashed curve*). (*B*) Effect of temperature on the ratio of excimer (479–488 nm) to monomer (394–397 nm) fluorescence intensity in the same liposomes as seen in *A*. (*C*) Repeat of the experiment shown in *B* in DPPC liposomes containing 0 mol % (□), 25 mol % (●), 30 mol % (∇), or 40 mol % (▼) cholesterol.

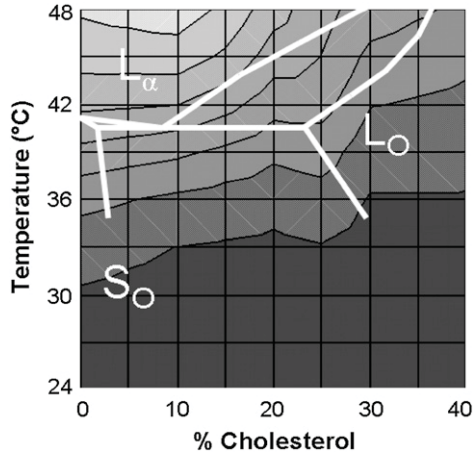

FIGURE 2 Relationship between bis-pyrene excimer/monomer ratio and a theoretical DPPC/cholesterol phase diagram. The data from Fig. 1 *C* were used to generate a contour plot as explained in Materials and Methods (contour lines represent increments of 0.11 units of excimer/monomer ratio) superimposed on an idealized phase diagram of DPPC and cholesterol (23).

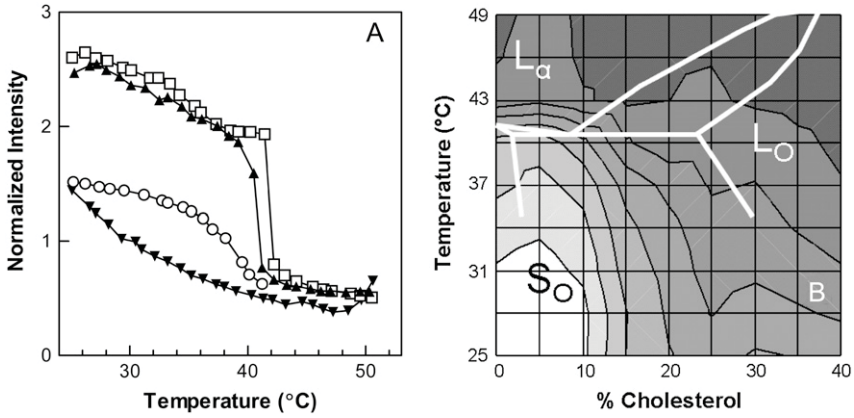

FIGURE 3 Effects of cholesterol and temperature on nystatin fluorescence intensity. Fluorescence emission spectra were obtained from liposomes composed of 0% (□), 10% (▲), 20% (○), or 40% (▼) cholesterol. Fluorescence intensity (404–412 nm) was normalized to the intensity measured at 50°C. The contour plot in *B* was generated as described in Materials and Methods, with lines representing 0.3-unit increments in normalized nystatin intensity.

centered at ~430 nm representing prodan partitioned into the membrane, and one at ~520 nm indicating free aqueous probe (Fig. 4 *A*, *solid curve*). Both peaks were replaced by an intermediate peak (~500 nm) when the lipids were in the L_α phase at high temperature (*dashed curve*). In the presence of 10% cholesterol (Fig. 4 *B*), the same pair of peaks was observed at low temperature, but the relative peak intensities were reversed (*solid curve*). The spectrum at high temperature and 10% cholesterol (Fig. 4 *B*, *dashed curve*) also had a shape similar to that obtained at the same temperature without cholesterol. At the highest cholesterol concentration (40%, Fig. 4 *C*), temperature affected the relative intensities of the two peaks but not the general spectral shape; i.e., similar to the low-temperature results in Fig. 4 *B*.

The changes in the shape of the prodan spectra were quantified by calculating the three-wavelength generalized polarization (3WGP, see Methods) to isolate the part of the spectrum defining membrane-associated probe. The plots of prodan 3WGP as a function of temperature and cholesterol concentration are displayed in Fig. 5 *A*. Effects of cholesterol concentration on the temperature dependence were more complex than with bis-pyrene or nystatin. These complexities revealed a contour plot that distinguished several of the regions defined by the DPPC/cholesterol phase diagram (Fig. 5 *B*). The most prominent feature of the data appeared to be sensitivity to the transition from ordered to disordered lipid as in the case of bis-pyrene in Fig. 2. In addition, the probe appeared to detect a transition in the pure DPPC sample in the vicinity of 34°C, well below the main phase transition. This additional transition is consistent with the so-called pretransition from the true S_O phase to the ripple phase (P'_β) (24,25).

Both the shape and the intensity of the MC540 emission spectrum were altered by temperature (Fig. 6 *A*). The shape of the spectrum was quantified by calculating the ratio of emission intensity at 585 nm to that at 621 nm. Fig. 6 *B* demonstrates that the ratio increased with temperature. As with prodan, the MC540 spectral shape in the pure DPPC sample was sensitive to temperature in a range suggestive of the pretransition to P'_β. The presence of low concentrations of cholesterol removed this apparent transition (Fig. 6 *B*). Beyond this effect, the temperature dependence was not affected significantly by cholesterol. The contour plot reinforced this observation (Fig. 7 *A*), again revealing that the only effect of cholesterol on MC540 fluorescence was to remove the low-temperature transition.

The lack of sensitivity to higher cholesterol concentrations was unexpected. To further verify this result, we repeated the MC540 analysis using steady state fluorescence anisotropy as a function of temperature and cholesterol content instead of emission spectra. As demonstrated in Fig. 7 *B*, MC540 revealed similar observations regardless of how the fluorescence was observed. This result is consistent with MC540 detecting membrane structural heterogeneity within the L_O phase.

DISCUSSION

Fluorescence spectroscopy has been used widely for many years to assess the level of fluidity in various artificial and biological membranes. There are several challenges in making such interpretations. For example, the term ''fluidity'' is often not well defined for phospholipid bilayers. It may refer to the average rate of lateral diffusion of membrane components. If measured using fluorescence anisotropy, it may refer to the average rotational diffusion rate for the membrane probe, or it may be defined by the orientational order parameter. Alternatively, it may refer to the degree of order among the phospholipid chains. In some cases, it may not be critical to make such distinctions when all of these parameters co-vary under certain experimental conditions such as the transition from S_O to L_α phases.

However, as more detailed information concerning the bilayer is sought, it becomes necessary to possess a better understanding of the experimental tools used. Given the convenience, ease, and experimental versatility of fluorescence spectroscopy, a solid understanding of the steady-state properties of various fluorescent probes seems worthwhile. Although the probes used in this study have been characterized and used extensively in the past to study membrane

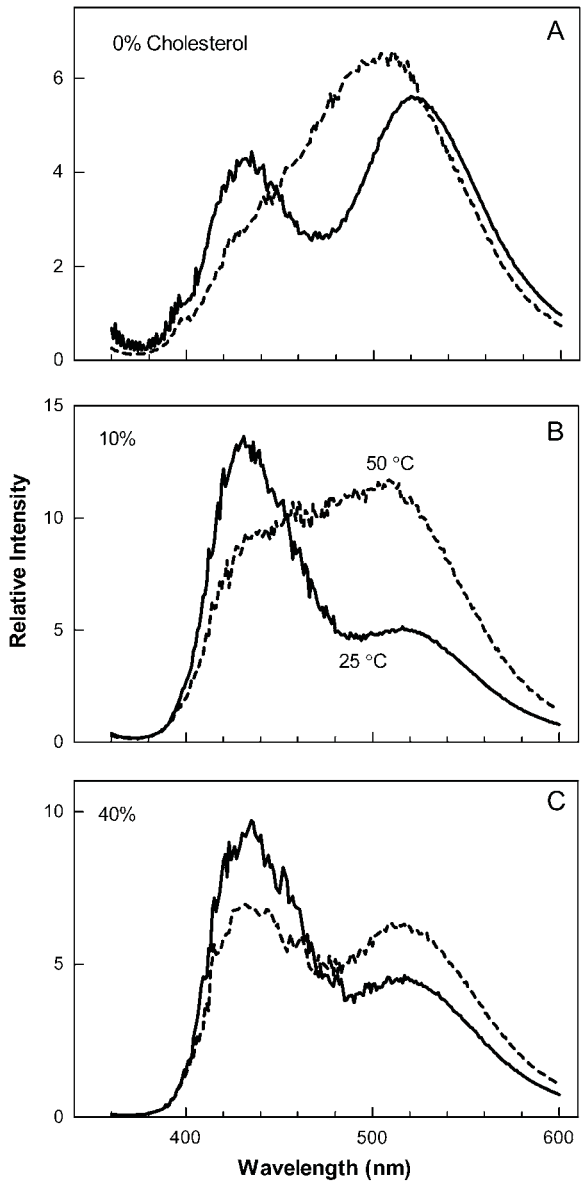

FIGURE 4 Effects of temperature and cholesterol on prodan emission spectra. (*A*) Prodan emission spectrum in liposomes composed of 100% DPPC at 25°C (*solid curve*) and at 50°C (*dashed curve*). The same conditions were used with liposomes containing 10% (*B*) or 40% (*C*) cholesterol.

phases, clear distinctions have not been made as to whether they detect lipid order, membrane fluidity, lipid packing, or some combination of the three. For the purposes of this study, we define ''order'' as representing conformational order of the phospholipid molecules (mostly based on the acyl chains in the experimental system used here), ''fluidity'' as representing the ability of lipids to diffuse in the plane of the bilayer and/or rotate, and ''packing'' as the spacing or distance between lipid molecules.

The L_O phase provides one means of making this distinction. In the simplest view, transitions between S_O and L_O phases should be detected by probes that sense membrane fluidity and be ignored by probes that primarily respond to chain order. The converse would be true for transitions from the L_O to the L_α phase. Furthermore, these studies are valuable because of their potential to identify fluorescent probes that can then be used to assess the presence of L_O-type domains in biological membranes. An example of this is Laurdan. Studies of the temperature dependence of Laurdan steady-state fluorescence in vesicles containing various mixtures of DPPC and cholesterol revealed that the emission spectra were sensitive mostly to lipid chain order. In contrast, the rate of Laurdan rotation in the membrane, assessed by steady-state anisotropy, was sensitive to both transitions from order to disorder as well as solid to liquid phase (2). Moreover, this information proved invaluable for interpreting changes in erythrocyte membrane structure upon treatment with calcium ionophore in a previous study (22). In those studies, experimental treatment appeared to increase the average order of membrane lipids (based on Laurdan emission spectra) while simultaneously producing a membrane that was more liquid (based on Laurdan anisotropy). Interpretation of the erythrocyte experiments would have been difficult had we not previously assessed the relationship between Laurdan fluorescence and the DPPC/cholesterol phase diagram.

It appears from the data of Fig. 2 that bis-pyrene senses transitions from ordered to disordered lipid but not the transition from the S_O to the L_O phase. Since bis-pyrene is immersed among the fatty acid chains, it is logical that disorder among those chains would allow the probe to vibrate freely and exhibit a high excimer probability. The insensitivity to the pure solid-liquid transition (i.e., between the S_O and L_O phases), however, was surprising. In fact, the probe has been used to study artificial and biological membranes in the past under the assumption that it detects fluidity (or ''microviscosity''; (4,26–29)). The results shown in Fig. 2 now require us to rethink that assumption. Careful perusal of the studies published in the past reveals that none of them included experiments capable of distinguishing changes in lipid order from changes in membrane fluidity. In fact, the studies in which the greatest care in quantifying the probe's sensitivity to microviscosity were conducted before the L_O phase and its distinctions from the S_O phase were well defined (4,26,27). Importantly, an early study by Melnick and colleagues (4) evaluating the ability of bis-pyrene to assess membrane fluidity used experiments similar to those of Fig. 1 *C* at 0% and 33% cholesterol. Their results were comparable to ours, but the interpretation was limited by the understanding of the day regarding membrane properties at low and high cholesterol concentrations. The explanation for why bis-pyrene is more sensitive to lipid order than fluidity (at least with respect to the DPPC/cholesterol phase diagram) may relate to the scale of movement involved. In the L_O phase, the rate of bulk diffusion of entire lipid molecules is increased relative to solid phases (2,30). In contrast, the smaller motions required for intramolecular excimer formation in bis-pyrene

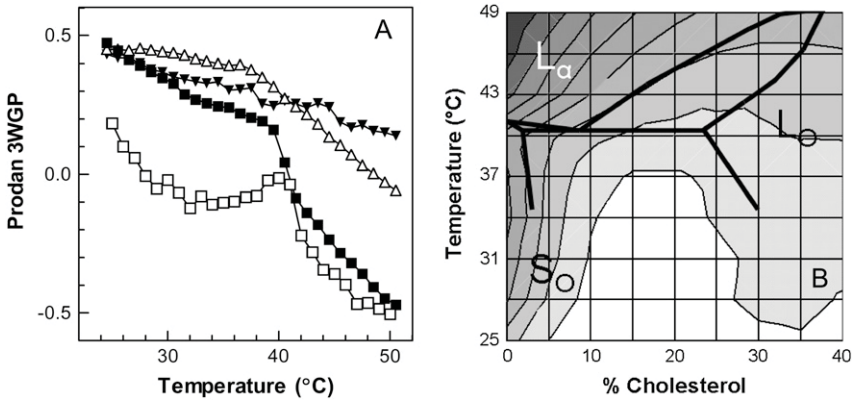

FIGURE 5 Relationship between prodan fluorescence the DPPC/cholesterol phase diagram. (*A*) 3WGP was calculated from spectra such as that in Fig. 4 for DPPC liposomes containing 0% (□), 5% (■), 15% (△), and 40% (▼) cholesterol. (*B*) Contour plot generated from the data in *A* as described in Materials and Methods, with lines representing increments of 0.11 units of prodan 3WGP.

are presumably restricted by interactions between the probe and ordered lipids. Pyrene derivatives that form intermolecular excimers are likely to detect true membrane fluidity since they require translational diffusion to interact with each other (3).

In contrast to bis-pyrene, nystatin appeared to detect transitions between solid and liquid phases while ignoring the level of chain disorder (Fig. 3). Specifically, when the membrane fluidity was low (i.e., in the S_O phase) the fluorescence intensity was high compared to emission from the L_α or L_O phases. This dependence of probe intensity on membrane phase corroborates previous findings (5,6,31). These and other observations have been interpreted as suggesting that the probe partitions differently into the bilayer when fluidity is high (based on measurements of nystatin fluorescence lifetimes (5,6), channel conductance, and theoretical considerations (32)). Emission under this condition is of low intensity because of alternate nonradiative relaxation pathways that involve changes in molecular vibrational states of the macrolide ring (6). In a solid-phase membrane, nystatin forms oligomers oriented deeper in the bilayer and parallel to the phospholipid chains (from depth-dependent quenching studies). Under this condition, fluorescence emission appears to be the primary path for the excited molecule back to ground state (6). Since phospholipid chain order appeared to have no effect on nystatin fluorescence intensity, we conclude that nystatin's placement in the membrane depends on the ability of lipids to diffuse laterally and not on the dynamics of the fatty acid chains. This conclusion disagrees with a previous statement that the disordered state of phospholipid acyl chains decreases partitioning of the probe into the membrane (5). However, those experiments were not capable of differentiating between membrane fluidity and chain order since comparisons were between S_O and L_α phases. When the same group considered the effects of cholesterol and ergosterol on nystatin partitioning, they observed a lack of effect of the sterols on that partitioning when the membrane contained mixtures of L_O and disordered phases, which substantiates the results in Fig. 3 (33). Furthermore, as shown in Fig. 8, we likewise obtained data with ergosterol that were nearly identical to those detected with cholesterol. This similarity between cholesterol and ergosterol identified by us and by others (31,33) reinforces the idea that it is the phase of the membrane that dictates effects of the sterols on nystatin fluorescence rather than specific lipid/probe interactions.

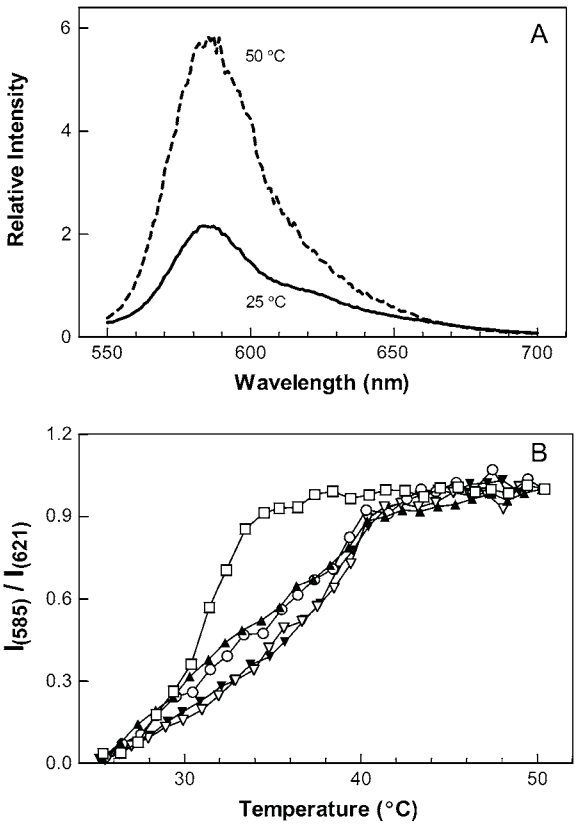

FIGURE 6 Effects of cholesterol and temperature on MC540 fluorescence. (*A*) MC540 emission spectrum in liposomes composed of 100% DPPC at 25°C (*solid curve*) and at 50°C (*dashed curve*). (*B*) Ratio of emission intensity calculated at 583–587 nm to that at 619–623 nm in DPPC liposomes containing 0% (□), 10% (▲), 20% (○), 30% (∇), or 40% (▼) cholesterol.

The probes that reside superficially in the membrane, prodan and MC540, detected membrane phenomena not

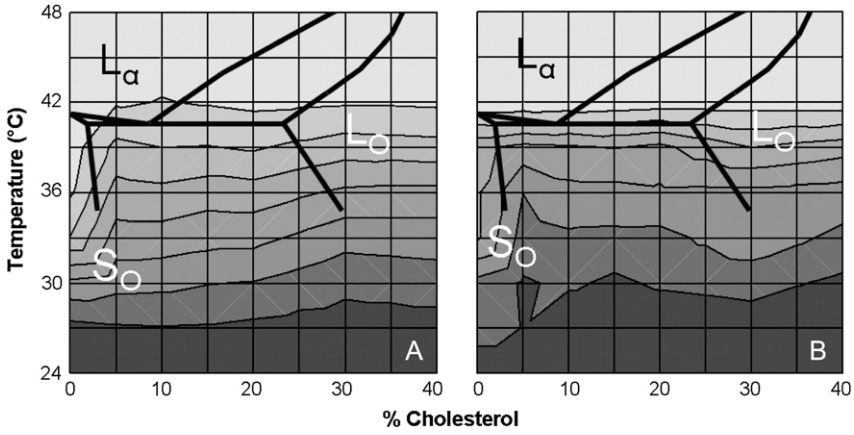

FIGURE 7 Relationship between MC540 fluorescence and the DPPC/cholesterol phase diagram. Contour plots were generated using the data from Fig. 6 *B* (*A*) or anisotropy measurements (*B*) as explained in Materials and Methods. Lines represent increments of 0.13 units of MC540 intensity ratio (*A*) or anisotropy (*B*).

visible to bis-pyrene and nystatin. One of these was the pretransition. This result is logical since the pretransition represents changes in the behavior of the phospholipid headgroups, the region occupied by prodan and MC540. The second difference was the presence of an apparent transition within the L_O phase. This apparent transition was the dominant result obtained with MC540. Prodan detected it weakly in addition to changes in both lipid order and fluidity.

The various alterations to the prodan emission spectrum illustrated in Fig. 4 led to a complex phase diagram (Fig. 5) in which contour lines appeared to follow all of the major phase boundaries (both order and fluidity). These results were consistent with previous observations of the behavior of prodan in different phases and can be explained based on the combined contributions of probe partitioning into the membrane and the solvent relaxation effect (34). Prodan partitions more strongly into liquid phases compared to solid phases. Thus, the peak representing free aqueous prodan (~520 nm) disappeared at temperatures above the main phase transition (Fig. 4 *A*). In addition, the spectral peak corresponding to membrane-bound prodan displayed a red-shift due to the solvent relaxation phenomenon (500 nm compared to 430 nm). The presence of low concentrations of cholesterol also improves prodan partitioning, presumably by increasing the spacing among phospholipids (35). Hence, the aqueous peak in Fig. 4 *B* was reduced in intensity compared to the membrane peak (430 nm) at low temperature with 10% cholesterol. At cholesterol concentrations >25% (Fig. 4 *C*), the structure of the L_O phase apparently maintained prodan partitioning at a level similar to that observed with the S_O phase regardless of temperature.

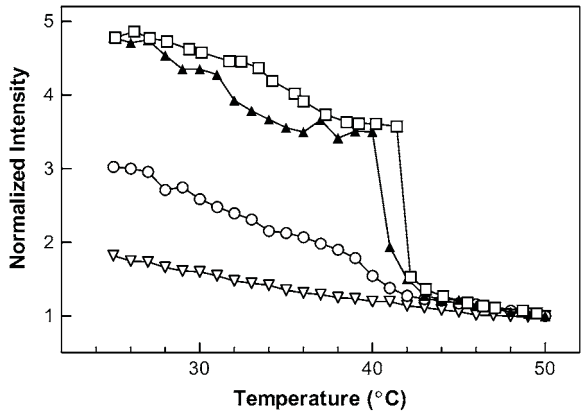

FIGURE 8 Effects of ergosterol and temperature on nystatin fluorescence intensity. The experiments of Fig. 3 were repeated using liposomes composed of DPPC and various concentrations of ergosterol: 0% (□), 10% (▲), 20% (○), and 30% (∇).

Three aspects of the temperature sensitivity of MC540 within the L_O phase (Fig. 7) were unexpected. First, the data suggested that cholesterol had no effect on the temperature dependence of the fluorescence of this probe (other than removal of the pretransition). Second, this sensitivity was greatest at the same temperature as the main solid-liquid phase transition in pure DPPC. Third, the other probes did not display a similar effect. A recent report analyzing diversity within the L_O phase detected by nuclear magnetic resonance and x-ray diffraction may help explain this result (36). Apparently, this diversity reflects melting of the phospholipid glycerol backbones at temperatures in the vicinity of 40°C at 40 mol % cholesterol (lower concentrations were not tested in that report). Of particular relevance, wide-angle x-ray scattering revealed an increase in the in-plane spacing of phospholipids in the same temperature range. Since MC540 resides superficially in the membrane and is sensitive to lipid packing (11–14), it seems likely that it would be sensitive to this phenomenon. Importantly, the data of Fig. 7 complement those of the previous study by demonstrating that this behavior occurs at all cholesterol concentrations within the L_O phase. In addition, the result underscores the fact that changes in lipid spacing or packing within the membrane do not always reflect concurrent changes in lipid order and/or fluidity.

Effective use of the data from all these probes is achieved by combining the contour plots of each into single displays (including Laurdan data obtained previously (2), as illustrated in Fig. 9. The data are organized with a primary color assigned according to the principal property observed with

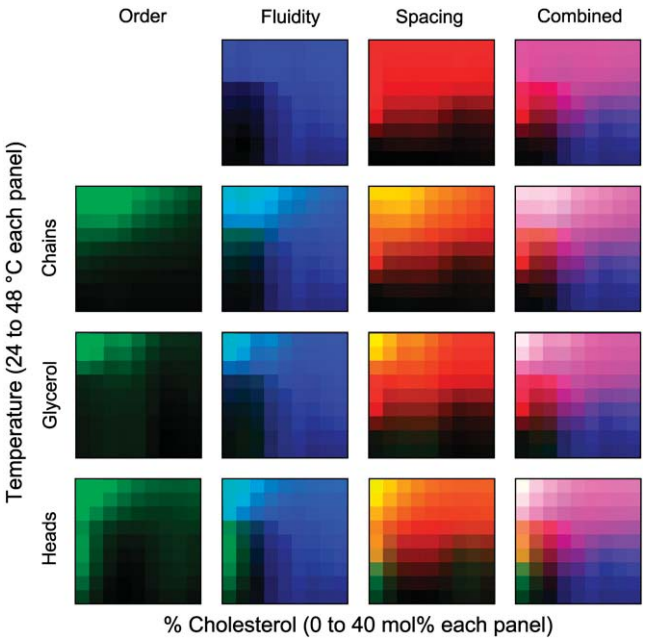

FIGURE 9 Combined contour plots revealing relative contributions of lipid order, fluidity, and spacing. The data from Figs. 2, 3, 5, and 7 *A*, together with results using the probe Laurdan from Harris et al. (2) were used to generate this figure. In each case, the data are represented by intensity of the color scaled to the fluorescence value from the corresponding figure at 24°C (*black*) to that at 48°C (full intensity) with pure DPPC. The ordinates in each panel represent temperatures ranging in 3°C increments from 24 to 48°C. The abscissas represent cholesterol contents in 5-mol % increments from 0 to 40 mol %. Green was used for probes that detect lipid order with increasing intensity, representing increasing disorder. The rows correspond to the various membrane depths represented by these probes; i.e., bis-pyrene (''chains''), Laurdan (''glycerol'' backbone), and prodan (''heads''). Blue was used for nystatin ''fluidity''. The top panel contains only the nystatin data. Each panel below in the same column contains the combined result of nystatin with the bis-pyrene, Laurdan, or prodan data. The same scheme applies to the third column for MC540 (*red*, ''spacing''). The fourth column represents (*top* to *bottom*) nystatin and MC540 data combined with either bis-pyrene, Laurdan, or prodan.

each probe; i.e., phospholipid order (bis-pyrene, Laurdan, prodan), lipid fluidity (nystatin), and lipid spacing (MC540). The intensity of the false color images reveals gradations in the indicated property quantitatively as in the contour plots with black representing the lowest value. Lipid order is shown in green in the left column. Because we have three different probes that measure lipid order at different levels along the length of the phospholipid molecule, three different graphs are presented (chains—bis-pyrene, glycerol backbone—Laurdan, heads—prodan). The blue and red panels in the top row summarize the data on fluidity (*blue*) and lipid spacing (*red*). The top right panel displays the consequence of overlaying the information regarding fluidity and lipid spacing. This overlay identifies regions of distinguishable properties not visible from either probe alone. This effect is enhanced when information regarding lipid order is included for different depths within the membrane (nine panels below first row). The bottom right panel combines the spacing and fluidity data with headgroup-order data. It provides the richest display of lipid-phase behavior and is expanded in Fig. 10, where eight distinct regions of lipid behavior in the phase diagram are labeled. Note that the colors are fairly stable in the left three regions (L_α, P'_β, and S_O) and in the right two regions (L_O(II) and L_O(I)). In contrast, the middle three regions are characterized by a smooth shift in color consistent with mixtures of two or more phases.

The distinction of these eight regions is significant since only six regions are included in previous complete phase diagrams (reviewed in Veatch and Keller (37). The two new regions are represented at subdivisions of the L_O phase into low (I) and increased (II) lipid spacing. Apparently, the mixed ordered phase region (S_O + L_O) also displays a similar subdivision.

The theoretical phase diagram used for comparison in the contour plots was chosen because it had been used previously for similar comparisons (2). However, this diagram does not necessarily represent the consensus of all researchers in the field. Specifically, there is disagreement as to whether there exists a true mixed phase region containing segregated domains of lipid in the L_α and L_O phases (as illustrated in the theoretical phase diagram in the contour plots) or whether there is a continuum of changes in lipid properties between the two phases with no clear boundary (reviewed in (37)). The results in Figs. 9 and 10 appear more consistent with the continuum model than one identifying distinct boundaries (identified as L_α~L_O(II) in the figure). Nevertheless, we recognize that fluorescence experiments are not the best choice for defining phase boundaries, because the presence of the probes as membrane contaminants obscures those boundaries. Studies using nuclear magnetic resonance, infrared spectroscopy, calorimetry, or x-ray diffraction

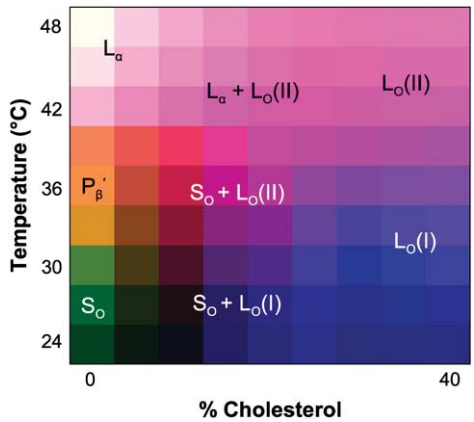

FIGURE 10 Summary of phase diagram regions identified by combined fluorescence of prodan (*green*), nystatin (*blue*), and MC540 (*red*). The data are from the lower right panel of Fig. 9. L_α, liquid-disordered phase; P'_β, rippled phase; S_O, solid-ordered phase; L_O(I), liquid-ordered phase with decreased lipid spacing; L_O(II), liquid-ordered phase with increased lipid spacing, L_α~L_O(II), undefined continuum between L_α and L_O phases.

are superior for that purpose. For example, recent experiments using pressure perturbation calorimetry suggest that the actual membrane structure in this region of the phase diagram displays characteristics intermediate between a continuum model and a phase separation model and that either model may be an adequate approximation of reality (38).

In addition to the gross designation of membrane phases such as L_α, L_O, and S_O, specific membrane structures have been described for cholesterol/phospholipid mixtures in greater molecular detail. These structures correspond to critical cholesterol/phospholipid mole ratios at which the geometric configuration of the lipids results in superlattice arrangements of the cholesterol molecules. At these critical mole fractions, the lipid packing is tighter, and fluidity and lipid order are also likely to be altered (31,39). In fact, data supporting this idea have been obtained using some of the same probes described in this article (i.e., MC540 and nystatin (31,39)) These structures cannot be discerned from the results presented in our study because insufficient cholesterol increments have been used. Furthermore, the magnitude of the fluorescence changes caused by superlattice structures are much smaller than those distinguishing the more general phases reported here. Nevertheless, given previous successes in studying these superlattice structures by fluorescence spectroscopy (31,39), it seems likely that application of the approach described in this article could be of value in exploring membrane properties in detail at the critical cholesterol mole fractions.

An important reason for using fluorescence spectroscopy is its applicability to studies of biological membranes where the other methods are more difficult or impossible to use. Advantages of steady-state fluorescence for such experiments include flexibility of experimental design, sensitivity, modest equipment requirements, the ability to conduct experiments in real time, and the possibility of gathering spatial information through microscopy. For example, numerous attempts have been made to use fluorescence spectroscopy to identify and quantify liquid-ordered structures in cell membranes (40–44). Accordingly, we used the approach summarized in Fig. 9 to examine properties of human erythrocytes (Fig. 11). Laurdan and MC540 data were obtained previously (20,21). We attempted to obtain data with nystatin; however, the probe did not bind sufficiently to erythrocyte membranes. Instead, we used anisotropy measurements with diphenylhexatriene, which provides fluidity information similar to that obtained with nystatin (because of changes in its rotational correlation time) in addition to reporting lipid order (see Fig. 11 and Vest et al. (22)). In our experience, the poor binding of bis-pyrene to erythrocytes is similarly problematic, and for that reason, it was also not used. Prodan was also not included because the probe binds to a number of proteins, which could potentially complicate the interpretation.

As revealed in Fig. 11, the average order and fluidity of the membrane appear to co-vary between 24° and 48°C, with the steepest temperature dependence occurring below 37°C (see

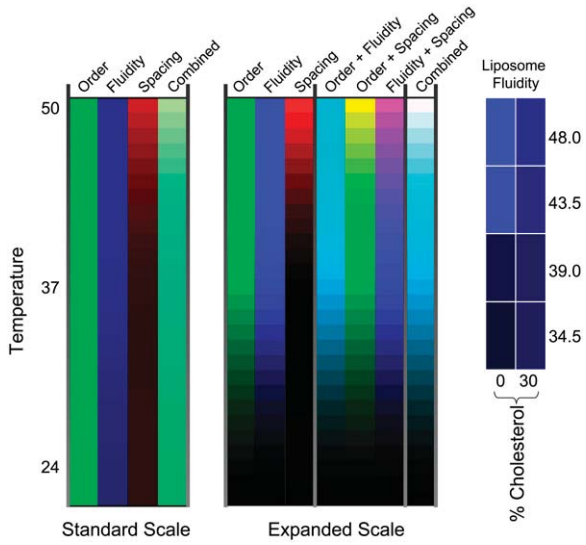

FIGURE 11 Fluorescence of Laurdan, diphenylhexatriene, and MC540 in human erythrocytes as a function of temperature. Laurdan data are shown in green (''disorder''), and were obtained from Best et al. (21). Diphenylhexatriene (*blue*, ''fluidity'') results were acquired as steady-state anisotropy, as described in Materials and Methods. The data were calibrated to the nystatin results using the S_O and L_α phases as standards (data for liposomes with 100% DPPC or 70% DPPC with 30% cholesterol are shown in the far right panel). MC540 data (*red*, ''spacing'') were obtained from Jensen et al. (20). In the left panel, the data are scaled as in Fig. 9 for comparison to liposomes. In the center panel, the data are scaled to the maximum and minimum signals in erythrocytes specific to each probe.

Expanded scale). Based on comparison to Fig. 9, the measured values of these properties were similar to those obtained for the L_α phase in the liposomes. This result is not surprising based on past experience and given the fact that the fatty acid chains of most aminophospholipids in biological membranes are unsaturated. In contrast, MC540 fluorescence, presumably reflecting lipid spacing, varied more extensively with temperature compared to that of the other two probes. Moreover, the temperature range at which changes in probe fluorescence were the greatest was different for MC540 compared to Laurdan and diphenylhexatriene (i.e., above 37°C rather than below). This theme of variation in apparent lipid spacing with temperature while order and fluidity remain nearly constant is reminiscent qualitatively of the type of behavior observed in the L_O phase in the liposomes, presumably reflecting the high cholesterol content of erythrocytes (45,46). The combined data suggest that the two regions of the DPPC/cholesterol phase diagram designated L_O(I) and L_O(II) apply qualitatively to the behavior of biological membranes. Determining whether they also apply quantitatively will be an interesting future direction to pursue using liposomes that more closely resemble cell membrane lipids. This approach also offers the possibility of examining the spatial distribution of properties in cell membranes using imaging techniques such as confocal fluorescence

microscopy or two-photon scanning microscopy, as has been done previously for erythrocytes using Laurdan (21,47).

In summary, our work reveals three important conclusions. First, prodan, nystatin, MC540, Laurdan, and bispyrene detect different properties associated with the lipid phases, and their combined use is applicable to studies of membrane physical behavior in living cells. Although none of these probes alone would provide conclusive evidence of any particular structure, such as those possessing L_O-type properties in uncharacterized membranes, the combination appears capable of identifying such structure. Second, the data reveal heterogeneity within the L_O phase that appears to relate to differences in lipid spacing. Third, similar behavior is observed as temperature is varied in a biological membrane with high cholesterol content. An exciting future step is to examine the fluorescence of these probes by microscopy and use the combined information to generate a spatial map of properties across the cell surface.

We gratefully acknowledge technical assistance from Rachel Bailey, Erin Olson, and Anna Solomon.

This work was supported by the National Science Foundation (MCB-9904597) and the National Institutes of Health (GM073997 and MH50003).

REFERENCES

1. Barenholz, Y. 2004. Sphingomyelin and cholesterol: from membrane biophysics and rafts to potential medical applications. *Subcell. Biochem.* 37:167–215.
2. Harris, F. M., K. B. Best, and J. D. Bell. 2002. Use of Laurdan fluorescence intensity and polarization to distinguish between changes in membrane fluidity and phospholipid order. *Biochim. Biophys. Acta.* 1565:123–128.
3. Galla, H. J., and E. Sackmann. 1974. Lateral diffusion in the hydrophobic region of membranes: use of pyrene excimers as optical probes. *Biochim. Biophys. Acta.* 339:103–115.
4. Melnick, R. L., H. C. Haspel, M. Goldenberg, L. M. Greenbaum, and S. Weinstein. 1981. Use of fluorescent probes that form intramolecular excimers to monitor structural changes in model and biological membranes. *Biophys. J.* 34:499–515.
5. Coutinho, A., and M. Prieto. 1995. Self-association of the polyene antibiotic nystatin in dipalmitoylphosphatidylcholine vesicles: a time-resolved fluorescence study. *Biophys. J.* 69:2541–2557.
6. Coutinho, A., and M. Prieto. 2003. Cooperative partition model of nystatin interaction with phospholipid vesicles. *Biophys. J.* 84:3061–3078.
7. Weber, G., and F. J. Farris. 1979. Synthesis and spectral properties of a hydrophobic fluorescent probe: 6-propionyl-2-(dimethylamino)naphthalene. *Biochemistry.* 18:3075–3078.
8. Chong, P. L., S. Capes, and P. T. Wong. 1989. Effects of hydrostatic pressure on the location of PRODAN in lipid bilayers: a FT-IR study. *Biochemistry.* 28:8358–8363.
9. Chong, P. L. 1988. Effects of hydrostatic pressure on the location of PRODAN in lipid bilayers and cellular membranes. *Biochemistry.* 27: 399–404.
10. Krasnowska, E. K., E. Gratton, and T. Parasassi. 1998. Prodan as a membrane surface fluorescence probe: partitioning between water and phospholipid phases. *Biophys. J.* 74:1984–1993.
11. Lelkes, P. I., D. Bach, and I. R. Miller. 1980. Perturbations of membrane structure by optical probes: II. Differential scanning calorimetry of dipalmitoyllecithin and its analogs interacting with Merocyanine 540. *J. Membr. Biol.* 54:141–148.
12. Lelkes, P. I., and I. R. Miller. 1980. Perturbations of membrane structure by optical probes: I. Location and structural sensitivity of merocyanine 540 bound to phospholipid membranes. *J. Membr. Biol.* 52:1–15.
13. Onganer, Y., and E. L. Quitevis. 1994. Dynamics of merocyanine 540 in model biomembranes: photoisomerization studies in small unilamellar vesicles. *Biochim. Biophys. Acta.* 1192:27–34.
14. Stillwell, W., S. R. Wassall, A. C. Dumaual, W. D. Ehringer, C. W. Browning, and L. J. Jenski. 1993. Use of merocyanine (MC540) in quantifying lipid domains and packing in phospholipid vesicles and tumor cells. *Biochim. Biophys. Acta.* 1146:136–144.
15. Williamson, P., K. Mattocks, and R. A. Schlegel. 1983. Merocyanine 540, a fluorescent probe sensitive to lipid packing. *Biochim. Biophys. Acta.* 732:387–393.
16. Yu, H., and S. W. Hui. 1992. Merocyanine 540 as a probe to monitor the molecular packing of phosphatidylcholine: a monolayer epifluorescence microscopy and spectroscopy study. *Biochim. Biophys. Acta.* 1107:245–254.
17. Langner, M., and S. W. Hui. 1993. Merocyanine interaction with phosphatidylcholine bilayers. *Biochim. Biophys. Acta.* 1149:175–179.
18. Bernik, D. L., and E. A. Disalvo. 1993. Gel state surface properties of phosphatidylcholine liposomes as measured with merocyanine 540. *Biochim. Biophys. Acta.* 1146:169–177.
19. Lagerberg, J. W., K. J. Kallen, C. W. Haest, J. VanSteveninck, and T. M. Dubbelman. 1995. Factors affecting the amount and the mode of merocyanine 540 binding to the membrane of human erythrocytes. A comparison with the binding to leukemia cells. *Biochim. Biophys. Acta.* 1235:428–436.
20. Jensen, L. B., N. K. Burgess, D. D. Gonda, E. Spencer, H. A. Wilson-Ashworth, E. Driscoll, M. P. Vu, J. L. Fairbourn, A. M. Judd, and J. D. Bell. 2005. Mechanisms governing the level of susceptibility of erythrocyte membranes to secretory phospholipase A2. *Biophys. J.* 88: 2692–2705.
21. Best, K., A. Ohran, A. Hawes, T. L. Hazlett, E. Gratton, A. M. Judd, and J. D. Bell. 2002. Relationship between erythrocyte membrane phase properties and susceptibility to secretory phospholipase A2. *Biochemistry.* 41:13982–13988.
22. Vest, R. S., R. Wallis, L. B. Jensen, A. C. Hawes, J. Callister, B. Brimhall, A. M. Judd, and J. D. Bell. 2006. Use of steady state Laurdan fluorescence to detect changes in liquid ordered phases in human erythrocyte membranes. *J. Membr. Biol.* 211:15–25.
23. Ipsen, J. H., O. G. Mouritsen, and M. J. Zuckermann. 1989. Theory of thermal anomalies in the specific heat of lipid bilayers containing cholesterol. *Biophys. J.* 56:661–667.
24. Janiak, M. J., D. M. Small, and G. G. Shipley. 1976. Nature of the thermal pretransition of synthetic phospholipids: dimyristolyl- and dipalmitoyllecithin. *Biochemistry.* 15:4575–4580.
25. Copeland, B. R., and H. M. McConnel. 1980. The rippled structure in bilayer membranes of phosphatidylcholine and binary mixtures of phosphatidylcholine and cholesterol. *Biochim. Biophys. Acta.* 599: 95–109.
26. Almeida, L. M., W. L. Vaz, K. A. Zachariasse, and V. M. Madeira. 1982. Fluidity of sarcoplasmic reticulum membranes investigated with dipyrenylpropane, an intramolecular excimer probe. *Biochemistry.* 21: 5972–5977.
27. Zachariasse, K. A., W. L. Vaz, C. Sotomayor, and W. Kuhnle. 1982. Investigation of human erythrocyte ghost membranes with intramolecular excimer probes. *Biochim. Biophys. Acta.* 688:323–332.
28. Mejia, R., M. C. Gomez-Eichelmann, and M. S. Fernandez. 1995. Membrane fluidity of *Escherichia coli* during heat-shock. *Biochim. Biophys. Acta.* 1239:195–200.
29. Mejia, R., M. C. Gomez-Eichelmann, and M. S. Fernandez. 1999. *Escherichia coli* membrane fluidity as detected by excimerization of dipyrenylpropane: sensitivity to the bacterial fatty acid profile. *Arch. Biochem. Biophys.* 368:156–160.
30. Almeida, P. F., W. L. Vaz, and T. E. Thompson. 1992. Lateral diffusion in the liquid phases of dimyristoylphosphatidylcholine/cholesterol lipid bilayers: a free volume analysis. *Biochemistry.* 31:6739–6747.

31. Wang, M. M., I. P. Sugar, and P. L. Chong. 1998. Role of the sterol superlattice in the partitioning of the antifungal drug nystatin into lipid membranes. *Biochemistry.* 37:11797–11805.

32. Helrich, C. S., J. A. Schmucker, and D. J. Woodbury. 2006. Evidence that nystatin channels form at the boundaries, not the interiors of lipid domains. *Biophys. J.* 91:1116–1127.

33. Coutinho, A., L. Silva, A. Fedorov, and M. Prieto. 2004. Cholesterol and ergosterol influence nystatin surface aggregation: relation to pore formation. *Biophys. J.* 87:3264–3276.

34. Krasnowska, E. K., L. A. Bagatolli, E. Gratton, and T. Parasassi. 2001. Surface properties of cholesterol-containing membranes detected by Prodan fluorescence. *Biochim. Biophys. Acta.* 1511:330–340.

35. Bondar, O. P., and E. S. Rowe. 1999. Preferential interactions of fluorescent probe Prodan with cholesterol. *Biophys. J.* 76:956–962.

36. Clarke, J. A., A. J. Heron, J. M. Seddon, and R. V. Law. 2006. The diversity of the liquid ordered (Lo) phase of phosphatidylcholine/cholesterol membranes: a variable temperature multinuclear solid-state NMR and x-ray diffraction study. *Biophys. J.* 90:2383–2393.

37. Veatch, S. L., and S. L. Keller. 2005. Seeing spots: complex phase behavior in simple membranes. *Biochim. Biophys. Acta.* 1746:172–185.

38. Heerklotz, H., and A. Tsamaloukas. 2006. Gradual change or phase transition: characterizing fluid lipid-cholesterol membranes on the basis of thermal volume changes. *Biophys. J.* 91:600–607.

39. Virtanen, J. A., M. Ruonala, M. Vauhkonen, and P. Somerharju. 1995. Lateral organization of liquid-crystalline cholesterol- dimyristoylphosphatidylcholine bilayers. Evidence for domains with hexagonal and centered rectangular cholesterol superlattices. *Biochemistry.* 34:11568–11581.

40. Gidwani, A., D. Holowka, and B. Baird. 2001. Fluorescence anisotropy measurements of lipid order in plasma membranes and lipid rafts from RBL-2H3 mast cells. *Biochemistry.* 40:12422–12429.

41. Scheiffele, P., A. Rietveld, T. Wilk, and K. Simons. 1999. Influenza viruses select ordered lipid domains during budding from the plasma membrane. *J. Biol. Chem.* 274:2038–2044.

42. Kindzelskii, A. L., R. G. Sitrin, and H. R. Petty. 2004. Cutting edge: optical microspectrophotometry supports the existence of gel phase lipid rafts at the lamellipodium of neutrophils: apparent role in calcium signaling. *J. Immunol.* 172:4681–4685.

43. Gaus, K., E. Gratton, E. P. Kable, A. S. Jones, I. Gelissen, L. Kritharides, and W. Jessup. 2003. Visualizing lipid structure and raft domains in living cells with two-photon microscopy. *Proc. Natl. Acad. Sci. USA.* 100:15554–15559.

44. Bacia, K., D. Scherfeld, N. Kahya, and P. Schwille. 2004. Fluorescence correlation spectroscopy relates rafts in model and native membranes. *Biophys. J.* 87:1034–1043.

45. Borochov, H., R. E. Abbott, D. Schachter, and M. Shinitzky. 1979. Modulation of erythrocyte membrane proteins by membrane cholesterol and lipid fluidity. *Biochemistry.* 18:251–255.

46. Parmahamsa, M., K. R. Reddy, and N. Varadacharyulu. 2004. Changes in composition and properties of erythrocyte membrane in chronic alcoholics. *Alcohol Alcohol.* 39:110–112.

47. Smith, S. K., A. R. Farnbach, F. M. Harris, A. C. Hawes, L. R. Jackson, A. M. Judd, R. S. Vest, S. Sanchez, and J. D. Bell. 2001. Mechanisms by which intracellular calcium induces susceptibility to secretory phospholipase A2 in human erythrocytes. *J. Biol. Chem.* 276: 22732–22741.